

# Are the effects of large scale flow conditions really lost through the turbulent cascade?

Gabriel G. Katul

Nicholas School of the Environment and Earth Sciences, Duke University, Durham, North Carolina, USA

Claudia Angelini, Daniela De Canditiis, and Umberto Amato

Istituto per le Applicazioni del Calcolo "Mauro Picone" - Napoli Section, Naples, Italy

Brani Vidakovic

School of Industrial and Systems Engineering, Georgia Institute of Technology, Atlanta, Georgia, USA

John D. Albertson

Department of Civil and Environmental Engineering, Duke University, Durham, North Carolina, USA

Received 8 April 2002; revised 25 May 2002; accepted 14 June 2002; published XX Month 2003.

[1] The conceptual framework for modeling the inertial subrange is strongly influenced by the Kolmogorov cascade phenomena, which is nowadays the subject of significant reinterpretation. It has been argued that the effects of boundary conditions influence large-scale motion and direct interaction between large and small scales is possible by means other than passing sequentially through the full cascade. Using longitudinal ( $u$ ) and vertical ( $w$ ) velocity and temperature ( $T$ ) time series measurements collected in the atmospheric surface layer ( $ASL$ ), we evaluate whether the inertial subrange multifractal function ( $f(\alpha)$ ) of all three flow variables is influenced by atmospheric stability ( $\xi$ ), which is a bulk measure of the effect of boundary conditions on large scale flow properties for  $ASL$  turbulence. This study is the first to demonstrate that  $\xi$  significantly influences  $f(\alpha)$  for all three flow variables. Here, statistical significance is evaluated using a novel wavelet-based Functional Analysis of Variance ( $FANOVA$ ) approach that explicitly considers different classes of  $\xi$ , the flow variable type, and possible interactions between  $\xi$  and the three flow variables. **INDEX TERMS:** 3250 Mathematical Geophysics: Fractals and multifractals; 3337 Meteorology and Atmospheric Dynamics: Numerical modeling and data assimilation; 3379 Meteorology and Atmospheric Dynamics: Turbulence. **Citation:** Katul, G. G., C. Angelini, D. De Canditiis, U. Amato, B. Vidakovic, J. D. Albertson, Are the effects of large scale flow conditions really lost through the turbulent cascade?, *Geophys. Res. Lett.*, 29(0), XXXX, doi:10.1029/2002GL015284, 2003.

## 1. Introduction

[2] The structure of turbulence in the inertial subrange has received much research attention over the past 50 years. This disproportionate interest is attributed to the possible emergence of universal or quasi-universal theories for turbulence [Schraiman and Siggia, 2000; Frisch et al., 1998], a research area of interest in many fields yet lacking a general theory to date. It is argued that any complete or general theory of turbulence must be capable of recovering

what is known about the inertial subrange structure thereby triggering such broad interest from many disciplines. The inertial subrange is loosely defined to encompass eddies much larger than the viscous dissipation scales yet much smaller than the integral length scale ( $L$ ) of the flow. The basic premise for the emergence of universal scaling is that the effect of large-scale anisotropic forcing or boundary conditions are rapidly lost during the cascade process thereby achieving local isotropy and universality at sufficiently smaller inertial scales [Biferale and Vergassola, 2001; Giostra et al., 2002]. However, results from numerical studies and experiments over the past decade suggest persistent effects of large scale anisotropies at these inertial scales even for very high Reynolds numbers and after many cascading steps [Warhaft, 2000; Celani et al., 2000; Antonov and Honkonen, 2001]. The departure from the so-called Kolmogorov [Kolmogorov, 1941] view of universal scaling and subsequent refinements [Kolmogorov, 1962] is supported by numerous observations of anomalous scaling in measured structure functions, particularly for passive scalars [Pumir and Shraiman, 1995; Sreenivasan and Antonia, 1997; Warhaft, 2000] and static pressure [Albertson, 1998]. The anomalous scaling for scalars is commonly attributed to short-circuiting of the energy cascade process due to the existence of organized large-scale features such as ramp-like structures, which are influenced by boundary conditions, and themselves directly influence small scale turbulence [Warhaft, 2000; Celani and Vergassola, 2001].

[3] To quantify whether boundary conditions influence the statistical properties of the inertial subrange for the atmospheric surface layer ( $ASL$ ), we estimate the inertial subrange multifractal function ( $f(\alpha)$ ) for longitudinal ( $u$ ) and vertical ( $w$ ) velocities, and temperature ( $T$ ) for three atmospheric stability ( $\xi$ ) classes: unstable, near-neutral, and stable. We proceed to assess whether these measures are significantly different across the flow variables and  $\xi$  classes. Hence, this analysis directly establishes whether a connection between the anisotropic large scale motion and inertial subrange scaling exists. The stability parameter  $\xi$  describes the combined influence of ground shear stress and surface heating (i.e. boundary conditions) on the larger-scale eddies for the  $ASL$ . Hence, any significant connection between  $\xi$

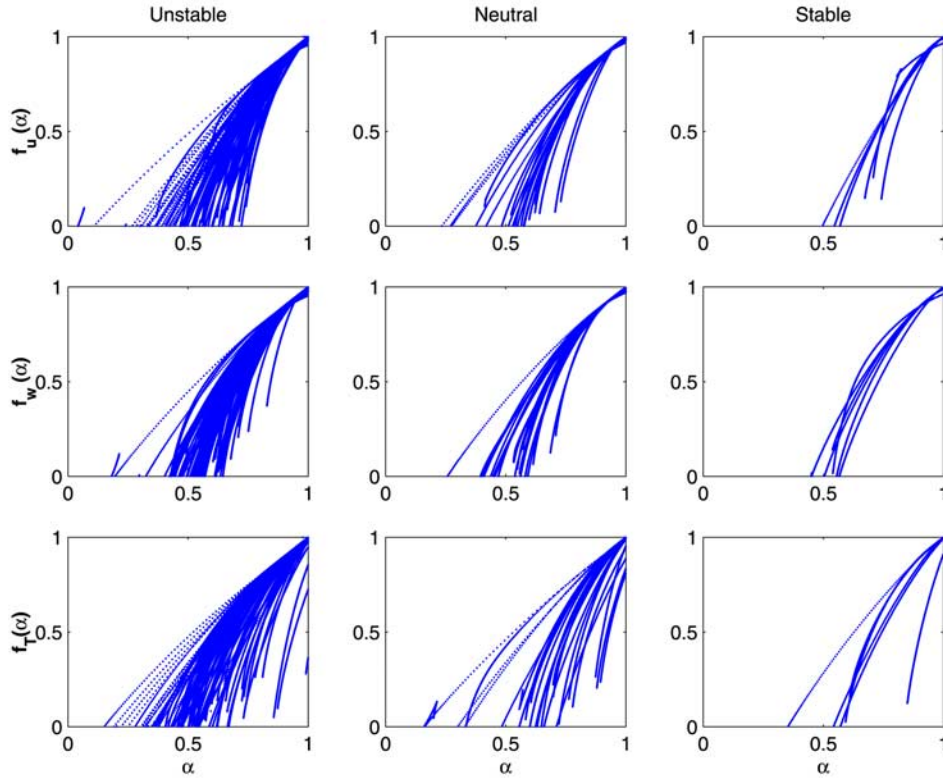


**Figure 1.** Estimated multifractal function  $f(\alpha)$  for  $u$  ( $= f_u(\alpha)$ ),  $w$  ( $= f_w(\alpha)$ ), and  $T$  ( $= f_T(\alpha)$ ), and for the threestability classes.

and scaling functions (e.g.,  $f(\alpha)$ ) in the inertial subrange must imply direct interaction between larger scales (influenced by  $\xi$ ) and inertial scales. The challenge then is to quantitatively describe the significance of the differences in  $f(\alpha)$  across the 3 flow variables and 3 stability classes. For significance testing, a wavelet-based Functional Analysis of Variance (FANOVA) approach is used to individually test for differences across stability classes and flow variable types, as well as for any potential interactions between them.

## 2. Multifractal Measures and Wavelets

[4] Consider any turbulent flow variable  $c$  along with its orthonormal wavelet image  $d(m, j)$ . The position index ( $j$ ) and scale index ( $m$ ) are defined using the standard multi-resolution format. The local energy  $e^{(m)}[j]$  at scale  $m$  and position  $j$  is defined as  $d^2$ . A relationship between the generalized dimension ( $D_q$ ) for the  $q$ th moment, the so-called singularity spectrum ( $f(\alpha)$ ), and the local scaling exponents ( $\alpha$ ) is given by [Meneveau, 1991; Meneveau and Sreenivasan, 1991]

$$\alpha = \frac{d}{dq}(q-1)D_q; \quad f(\alpha) = q\alpha - (q-1)D_q \quad (1)$$

[5] From the wavelet coefficients, the set of scaling exponents  $D_q$  can be estimated by [Meneveau, 1991]

$$\langle e^{(m)}[j]^q \rangle \sim \langle (e^{(m)}[j]) \rangle \left( \frac{r_m}{L} \right)^{(q-1)(D_q-D)} \quad (2)$$

where  $r_m = 2^m dx$  is the scale,  $dx$  is the sampling increment,  $L$  is the integral length scale,  $\langle \cdot \rangle$  is averaging

over the position index  $j$ , and  $D$  is the dimension of the embedding space ( $D = 1$  for one dimensional cuts through the flow).

[6] A plot of  $\alpha$  (independent) versus  $f(\alpha)$  (dependent) is often referred to as the multifractal (Legendre) spectrum of  $c$ . These functions are computed for  $u$ ,  $w$ , and  $T$  for unstable, stable, and near neutral conditions using the data sets described next. An important difference between the multifractal formalism classically employed for turbulent kinetic energy dissipation rates and the derivation above is that the former is employed for conservative cascades while the latter is not. The mean dissipation represents the net flux of kinetic energy from large to small scales independent of scale (or  $r_m$ ). On the other hand, the multifractal formalism used above characterizes the intermittency of the energy around its scale dependent mean value. Such a definition is more closely related to the multifractal formalism first introduced by Parisi and Frisch [Frisch, 1995].

## 3. Data

[7] Time series measurements of  $u$ ,  $w$ , and  $T$  were sampled at 56 Hz and at 5.2 m above a grass surface at Duke Forest near Durham, North Carolina. We focus on an ensemble of 103 runs collected over a wide range of  $\xi$  ranging from near convective to stable atmospheric flows. The ensemble size of all combined runs exceeds  $6.75 \times 10^6$  time measurement (but the analysis is conducted on individual 19.5 minute runs prior to ensemble averaging). The time series was converted to space using the frozen turbulence hypothesis. Further details can be found elsewhere [Katul et al., 1997; Katul et al., 2000]. To assess the effects

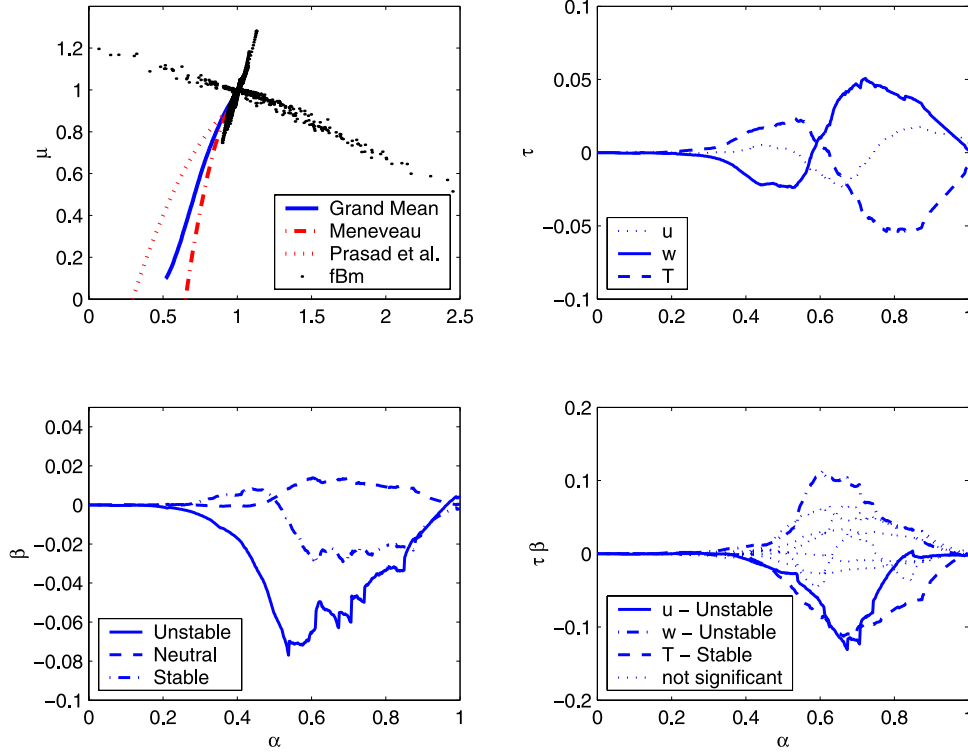


**Figure 2.** The application of *FANOVA* to the  $f(\alpha)$  data in Figure 1. Upper left panel is the computed grand mean for all stability classes and all three flow variable type. For comparison, we show the  $f(\alpha)$  derived from turbulent kinetic energy dissipation rate measurements reported in *Meneveau* [1991] and the  $f(\alpha)$  derived from scalar concentration fluctuation dissipation rates reported in *Prasad et al.*, [1988]. We also show the ensemble  $f(\alpha)$  computed for 103 *fBm* runs (in dots). Upper-right panel represents the functions associated with the flow variable type ( $u$ ,  $w$ , and  $T$ ). The significant ones (i.e. scalar type  $w$ ,  $T$ ) are plotted as bold lines. Lower-left panel shows all significant effect functions for the stability classes. Lower-right panel depicts 9 interactions; 3 that are found to be significant are described in the Figure legend. Significance is tested at the 5 level throughout.

of finite sampling duration on the estimation of  $f(\alpha)$ , we repeated all the calculations for 103 fractional Brownian motion (*fBm*) time series runs, each of sample size  $N = 65,536$  and a Hurst exponent =  $1/3$ . To perform the comparisons with these simulated *fBm* time series, each velocity and temperature run was normalized to zero-mean and unit variance prior to the estimation of  $D_q$ .

## 4. Results and Discussion

### 4.1. Estimation of $f(\alpha)$ for $u$ , $w$ , and $t$

[8] The resulting  $f(\alpha)$  for unstable, stable, and near-neutral conditions for each variable ( $u$ ,  $w$ , and  $T$ ) are shown in Figure 1. Unstable atmospheric conditions are defined for  $-\xi > 0.05$ , near neutral conditions for  $\langle \xi \rangle < 0.05$ , and stable conditions for  $\xi > 0.05$ . There were 74 unstable, 23 neutral, and 6 stable runs, respectively. The  $f(\alpha)$  were evaluated for  $q \in [0, 4]$  in 0.02 increments. The order of the moment  $q$  increases when one moves along the spectra from the upper right part to the lower left part in Figure 1. The Daubechies 4-tap wavelet filter and boundary-corrected wavelets are used throughout.

### 4.2. Significance Tests Using *FANOVA*

[9] The computed  $f(\alpha)$  can be represented by a functional ANOVA (Analysis of Variance) model (e.g., [Ramsay and Silverman, 1997]), given by

$$f_{ijk}(\alpha) = \mu(\alpha) + \tau_i(\alpha) + \beta_j(\alpha) + (\tau\beta)_{ij}(\alpha) + \varepsilon_{ijk}(\alpha);$$

$$i = 1; \dots; 3; j = 1; \dots; 3; \text{ and } k = 1; \dots; n_{ij};$$

where  $\alpha$  is restricted to  $[0, 1]$ . Functions  $\mu(\alpha)$ ,  $\tau_1(\alpha)$ ,  $\dots$ ,  $\tau_3(\alpha)$ ,  $\beta_1(\alpha)$ ,  $\dots$ ,  $\beta_3(\alpha)$ ,  $(\tau\beta)_{11}(\alpha)$ ,  $\dots$ ,  $(\tau\beta)_{33}(\alpha)$ , represent the so-called *grand mean*, choice of variable  $u$ ,  $w$ , and  $T$  (hereafter referred to as treatment effects of the source), effects of the stability classes *unstable*, *neutral*, and *stable*, and 9 interactions between the 3 flow variables and the 3 stability classes, respectively. These functions define the components of  $f_{ijk}(\alpha)$ . Errors  $\varepsilon_{ijk}(\alpha)$  are assumed normal and independent with respect to  $i, j$ , and  $k$ , but dependent for different values of  $\alpha$ . The estimation and testing of these components is briefly described next. To ensure equal support and equispaced data, discretely measured  $f_u(\alpha)$ ,  $f_w(\alpha)$  and  $f_T(\alpha)$  for each run are first binned to 512 equal intervals in  $[0, 1]$ , and the binned averages, taken as value points, are transformed into the wavelet domain. The *FANOVA* in the wavelet domain was performed to separate the components (i.e., grand mean, treatment effects, and all 9 interactions). The inverse wavelet transformation is then applied to the regularized wavelet coefficients to recover these components in physical space. The regularization utilized Lorentz wavelet thresholding, shown to be optimal for the analysis of surface layer turbulence [Katul and Vidakovic, 1998]. The inference was performed as follows: The

regularized coefficients corresponding to all the component functions are standardized by the pooled estimator of their variances. The total energy of the standardized coefficients, approximately distributed as a  $\chi^2$ , was used to assess significant deviations from the null function (e.g., [Fan and Lin, 1998]). Unlike the traditional ANOVA, which tests simultaneously equality to 0 of effects and interactions, the *FANOVA* is capable of testing these equalities individually.

[10] In Figure 2, the computed grand mean is presented along with two-bounds: the  $f(\alpha)$  derived from turbulent kinetic energy dissipation rate measurements reported in [Meneveau, 1991] and the  $f(\alpha)$  derived from two-dimensional scalar concentration fluctuation dissipation rates reported in [Prasad et al., 1988]. The source effect suggest that both  $w$  and  $T$  are found to be significant. The lower-left